Harmonic Analysis of Time-Series NOAA/AVHRR Images for Hotspot Detection and Land Features Classification

R. S. Gautam, D. Singh, A. Mittal
Department of Electronics & Computer Engineering
Indian Institute of Technology Roorkee
Roorkee, India
{rsgcsdec, dharmfec, ankumfec}@iitr.ernet.in

S. Bhatia
Department of Electrical Engineering
Indian Institute of Technology Roorkee
Roorkee, India
sumi1uee@iitr.ernet.in

***Abstract*—In this paper, Harmonic analysis of 10-year time series (1995-2005) NOAA/AVHRR yearly composite images is performed to develop an innovative technique for hotspot detection and land-features classification based on temporal changes in the NDVI and various AVHRR band values. NOAA/AVHRR images are used due to wide coverage, high frequency and free acquisition offered by NOAA/AVHRR sensors. Proposed algorithm consists of three steps: (1) preprocessing of NOAA/AVHRR images to correct geometric distortions and calibrate the data radiometrically, (2) detection of cloud and water pixels in the preprocessed image and application of harmonic analysis on 10-years time series AVHRR images to produce phase and amplitude images, and (3) application of image processing techniques on the amplitude images of different bands to detect hotspots and classify the region of interest. The obtained results indicate that the proposed method can classify the region of interest successfully with through out greater than 91% classification accuracy.**

Keywords-harmonic analysis; NOAA/AVHRR; hotspot; time-seris; image processing

I. INTRODUCTION

Several countries in the world are facing the problem of surface and subsurface coal fires (hotspots) and lots of efforts are being paid in this direction for detecting and monitoring these hotspots. Since, ground based monitoring of these hotspots is very expensive and cumbersome, attention is being paid towards exploiting the potential of the satellite imaging in order to develop an economic and promising solution for the same. Several methods have been proposed for surface and subsurface fire detection [1, 2] but they lack in providing economic solution as the satellites data used in these study are quite expensive. Therefore it is the current need of research to use such satellite data which can be freely available and can effectively be utilized for the present problem.

The satellite images used in this study were acquired from NOAA (National Oceanic and Atmospheric Administration) satellite's AVHRR (Advanced Very High Resolution Radiometer) sensor. NOAA/AVHRR images exhibit good temporal resolutions and are freely acquired and thus, are the most suitable option for hotspot detection.

Several researchers have taken the advantage of time-series analysis of NOAA/AVHRR data for different purposes [3-5]. In this paper, the time series data are used for classification based on the temporal characteristics of the images. Harmonic analysis of 10-years time series NOAA/AVHRR yearly composite images has been performed in order to detect hotspots and classify the region of interest in major classes i.e. deemed land, water and medium forest land. The proposed method takes into account the temporal changes in the NDVI (normalized difference vegetation index) and various AVHRR band values to achieve the objective.

II. STUDY AREA AND SATELLITE DATA

A. Study Area

The study was carried out in the Jharia coalfield region of Jharkhand, India. The region is bounded by Latitude (N) $22^{\circ}00'00''$ to $24^{\circ}00'0''$ and Longitude (E) $85^{\circ}00'00''$ to $87^{\circ}00'00''$. There are several subsurface fires (more than 70) existing in this region which are burning from several decades [6]. These fires lead to degradation of land and do not allow any vegetation to grow in the area.

B. Satellite Data

The satellite data used in this study were AVHRR onboard the NOAA satellite series level 1B. NOAA/AVHRR image comprises five spectral bands: visible (ch.1, 0.63 μm), near-infrared (ch.2, 0.83 μm), mid-infrared (ch.3, 3.75 μm), and thermal (ch.4-5, 10-12 μm). The nominal spatial resolution of AVHRR is 1.1 kilometer at nadir. For our study NOAA/AVHRR data were collected for the month of February, in between the period of year 1995-2005. The type of each data is AVHRR- Local Area Coverage (LAC).

C. Auxiliary Data

The obtained results from of the proposed algorithm were validated by ground truth information provided by BCCL (Bharat Coaking Coal Limited) which include the place and location of 30 hotspots in Jharia region. In addition, co-registered "Google Earth" image [7] was used to validate the land-cover classification results.

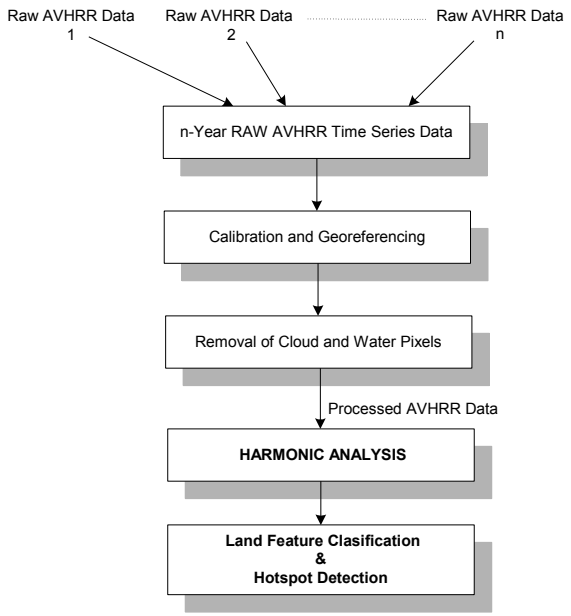

Figure 1. Flow chart of the proposed algorithm.

III. METHODOLOGY

The flow chart of the proposed algorithm is shown in Fig. 1. Each step of the algorithm is discussed in detail in following subsections:

A. Preprocessing

Radiometric calibration followed by georeferencing of NOAA/AVHRR images is carried out using commercially available software ENVI. First two bands (band 1 and 2) are in % reflectance, and bands 3, 4, and 5 are in brightness temperature.

B. Harmonic Analysis of Time-Series NOAA/AVHRR Data

The cloudy pixels are removed by applying the cloud detection technique as described in [8]. Normalized Difference Vegetation Index (NDVI) is used to identify water pixels in the input image.

NDVI is defined as [9]

$$\mathrm{NDVI} = \frac{\rho_2 - \rho_1}{\rho_2 + \rho_1} \tag{1}$$

where ρ_1 and ρ_2 are TOA (top of atmosphere) reflectances in channel 1 and channel 2 respectively. Pixels, for which corresponding NDVI value is less than zero, are marked as water pixels.

In this paper, harmonic analysis, also known as Fourier analysis, is used to decompose a time dependent periodic phenomena into a series of sinusoidal functions, each defined by a unique amplitude and phase value. The details of the harmonic analysis technique can be found in [4].

Harmonic analysis of a 10-year time series NOAA/AVHRR data is carried out for the purpose of Hotspot detection and land cover classification in Jharia region of Jharkhand. It is assumed that hotspot pixels exhibit low reflectance value in comparison to the background pixels in AVHRR channels 1 and 2 [10, 11]. In addition, highly reflective bare soil and rock are one of the largest sources of false hotspot detection [10, 11] and channel 2 reflectance is used to eliminate these potential false alarms. NDVI also plays very important role in hotspot detection and land features classification [3, 5]. It is assumed that in the hotspot area, vegetation will be very less, exhibiting lower NDVI value. Hence, taking into account the aforementioned facts, AVHRR channel 1, channel 2 and NDVI are taken as input for hotspot detection and land features classification.

The technique of harmonic analysis is applied to the band 1, band 2 and NDVI of AVHRR time series data, on a pixel by pixel basis. In this way Fourier analysis of the whole image is carried out resulting amplitude and phase images for each term. Since, the majority of the variance in a data set is contained in

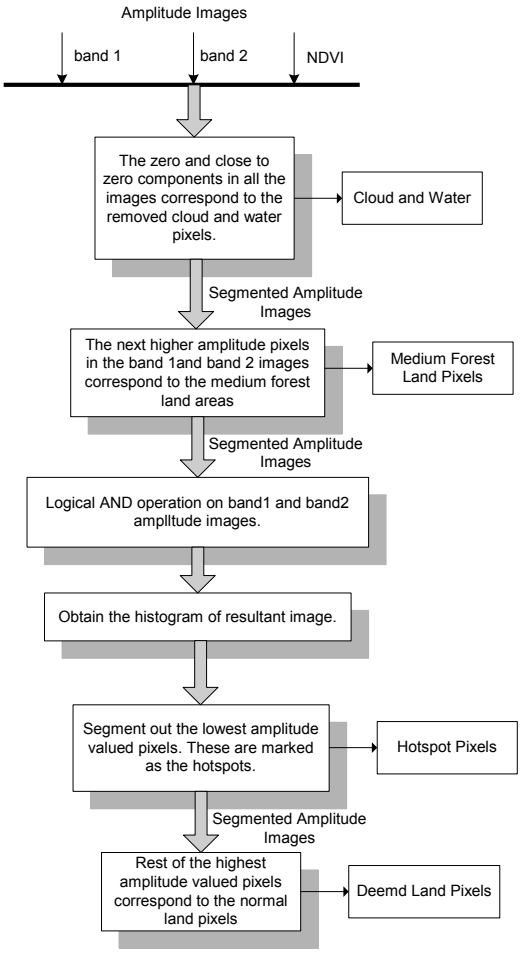

Figure 2. Flow chart of the process of identifying cloud and water pixels in NOAA/AVHRR image.

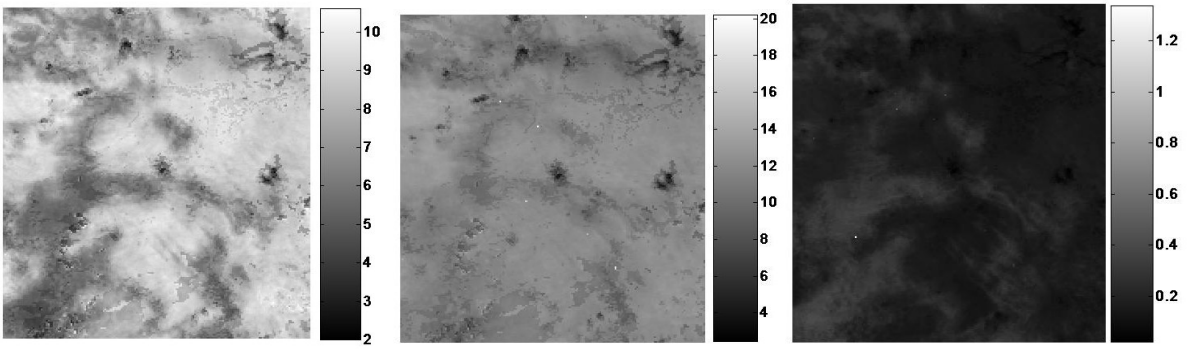

(a) (b) (c)

Figure 3. Fundamental amplitude images of band 1 (a), band 2 (b) and NDVI (c).

the first few terms (components); amplitude images for the fundamental harmonic terms are extracted and used for further analysis.

C. Application of Image Processing Techniques

The obtained amplitude images of fundamental term corresponding to band 1, band 2 and NDVI show unique characteristics for different land features i.e., land, water, and medium forest land and hence enable us to classify these land covers and detect the hotspots successfully. To achieve the objective, image processing techniques are applied to the extracted amplitude images and different land-covers are segmented out using the process shown in Fig. 2.

The zero and close to zero valued pixels correspond to the cloud and water pixels in all of the amplitude images as they were already masked in all 10-years of the AVHRR images using the method discussed in section III (B), and hence are easily segmented out. The medium forest land pixels in the area of interest exhibit low reflectance value in channel 1 images and high pixel value in NDVI images. Therefore medium forest land pixels exhibit lowest response also in the resulting channel 1 amplitude image and highest response in NDVI amplitude image and thus, are segmented out based on these characteristics.

After performing the aforementioned segmentations, the resulting image contains only deemed land pixels and hotspots pixels. Since hotspot pixels show low reflectance values in comparison to deemed land pixel in both AVHRR band 1 and band 2, hence the amplitude values corresponding to the hotspot pixels are lower than the background land pixels which is also verified in channel 1 and channel 2 resultant amplitude images using ground truth information (provided by BCCL) of hotspots. Therefore a proper processing of the two images yields the desired result as described below.

After segmenting out water, cloud, and medium forest land pixels, logical AND operation is performed on band 1 and band 2 amplitude images in order to exploit the hotspot information contained in both images. Then a histogram of the resulting image is obtained and with the help of that, the lowest responsive pixels are segmented out from the amplitude images. These identified pixels are marked as hotspots. The rest of the image pixels which exhibit highest response in both amplitude images of channels 1 and 2, are marked as land pixels.

IV. RESULTS AND DISCUSSION

Fig. 3 shows the amplitude images corresponding to band 1, band 2 and NDVI (refer to Fig. 3a, 3b and 3c respectively), obtained after applying harmonic analysis on 10-years time series NOAA/AVHRR yearly composite images of Jharia region. From these images it can be seen that different land covers i.e., water, land and medium forest land exhibit unique characteristics as mentioned in section III (C) which help to discriminate them from rest of the image pixels.

Fig. 4 shows the annotated classified image obtained after applying image processing techniques on the amplitude images as discussed in section III (C). The image has been classified primarily in four classes i.e., water and cloud, medium forest land, hotspot and land pixels.

In order to analyze the performance of proposed hotspot detection and land-cover classification algorithm, we computed the confusion matrix for each class using ground truth information of hotspots (provided by BCCL) and co-registered

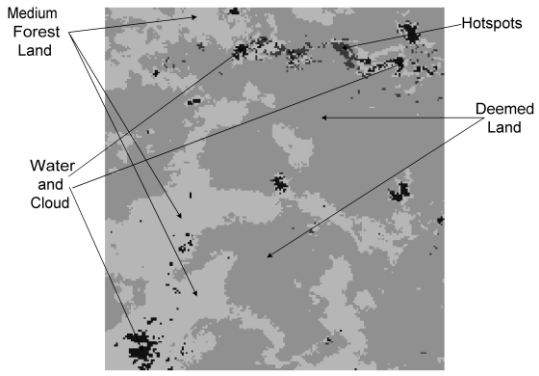

Figure 4. Final annotated classified AVHRR image in four major classes.

TABLE I. CONFUSION MATRIX FOR HOTSPOT CLASS

Hotspots	*Predicted Positive*	*Predicted Negative*
Actual Positive	25 (TP)	0 (FN)
Actual Negative	310 (FP)	37641 (TN)

TABLE II. CONFUSION MATRIX FOR MEDIUM FOREST LAND CLASS

Medium Forest Land	*Predicted Positive*	*Predicted Negative*
Actual Positive	10081 (TP)	0 (FN)
Actual Negative	3066 (FP)	24829 (TN)

TABLE III. CONFUSION MATRIX FOR DEEMED LAND CLASS

Deemed Land	*Predicted Positive*	*Predicted Negative*
Actual Positive	24176 (TP)	3376 (FN)
Actual Negative	14 (FP)	10410 (TN)

TABLE IV. CONFUSION MATRIX FOR WATER CLASS

Water	*Predicted Positive*	*Predicted Negative*
Actual Positive	290 (TP)	14 (FN)
Actual Negative	0 (FP)	37672 (TN)

Google earth image [7]. From the confusion matrices classification accuracy was calculated defined as:

$$\text{Classification Accuracy} = \frac{\text{TP} + \text{TN}}{\text{Total no. of pixels}} \qquad (2)$$

where TP (true positive) is the number of pixels correctly classified in that particular class and TN (true negative) is the number of pixels correctly classified in other classes. Tables I, II, III, and IV show the confusing matrices computed for each of the classes. The overall classification accuracy of the whole classified image was determined as defined below:

$$\text{Overall classification accuracy} = \frac{\text{TP (Hotspots)} + \text{TP (Hills)} + \text{TP (Land)} + \text{TP (Water)}}{\text{Total Number of pixels in the image}} \qquad (3)$$

Table V shows the classification accuracy calculated for each class and the classification accuracy of the whole AVHRR classified image. From the table it is clear that proposed algorithm was able to detect all of the hotspots and classify the region of interest in different land-covers successfully. The overall classification accuracy obtained was 91.04% which shows the significant achievement of the algorithm.

TABLE V. CLASSIFICATION ACCURACY COMPUTED FOR EACH CLASS AND THE OVERALL CLASSIFICATION ACCURACY

Classes	Classification Accuracy (%)	Overall Classification Accuracy (%)
Hotspots	99.18	91.04
Medium Forest Land	91.93	
Deemed Land	91.07	
Water	99.96	

V. CONCLUSION

An algorithm was proposed for hotspot detection and land-cover classification of the Jharia coalfield region of India. To achieve the objective, harmonic analysis of 10-year time series (1995-2005) NOAA/AVHRR yearly composite images was performed. Image processing techniques were applied to detect the hotspots in frequency domain and segment out the amplitude images of the region of interest in different land-over classes. The obtained results indicate that the proposed algorithm worked successfully and detected most of the hotspots successfully. In addition, the algorithm was also able to classify the region of interest with 91.04% accuracy.

REFERENCES

[1] A. Prakash, R. P. Gupta, and A. K. Saraf, "A Landsat TM based comparative study of surface and subsurface fires in the Jharia coalfield, India," Int. J. Rem. Sens., vol. 18, pp. 2463-2469, 1997.

[2] A. Prakash and R. P. Gupta, "Surface fires in Jharia coalfield, India – their distribution and estimation of area and temperature from TM data," Int. J. Rem. Sens., vol. 20, pp. 1935-1946, 1999.

[3] S. L. Egbert, M. Ortega-Huerta, E. Martinez-Meyer, K. P. Price, and A. T. Peterson, "Time-series classification of high-temporal resolution AVHRR NDVI imagery of Mexico," IEEE International Geoscience and Remote Sensing Symposium, vol. 5, pp. 1978-1980, 2000.

[4] M. E. Jakubauskas, D. R. Legates, and J. H. Kastens, "Harmonic analysis of time-series AVHRR NDVI data," Photogramm. Eng. Remote Sensing, vol. 67, pp. 461-470, 2001.

[5] S. Liang, "Land-cover classification methods for multi-year AVHRR data," Int. J. Rem. Sens., vol. 22, pp. 1479-1493, 2001.

[6] R. Agarwal, D. Singh, D. S. Chauhan, and K. P. Singh, "Detection of coal mine fires in the Jharia coal field using NOAA/AVHRR data," J. Geophys. Eng., vol. 3, pp. 212-218, 2006.

[7] Google Earth. Available at: http://earth.google.com/earth.html, 2005.

[8] Z. Li, A. Khananian, R. H. Fraser, and J. Cihlar, "Automatic detection of fire smoke using artificial neural networks and threshold approaches applied to AVHRR imagery," IEEE Trans. Geosci. Rem. Sens., vol. 39, pp. 1859-1870, 2001.

[9] D. Singh, G. A. Costa, M. S. Meirelles, I. Herlin, J. P. Berroir, and E. F. Silva, "A methodology to support environmental degradation monitoring and analysis using AVHRR data," Anais XII Simpósio Brasileiro de Sensoriamento Remoto, Goiânia, Brasil, INPE, pp. 2941-2948, 2005.

[10] L. Giglio, J. D. Kendall, and C. O. Justice, "Evaluation of global fire detection algorithms using simulated AVHRR infrared data," Int. J. Rem. Sens., vol. 20, pp. 1947-1985, 1999.

[11] P. J. Kennedy, A. S. Belward, J. Grègoire, "An Improved Approach to Fire Monitoring in West Africa Using AVHRR Data," Int. J. Rem. Sens., vol. 15, pp. 2235-2255, 1994.